Chapter 2
Topology and Geometry in Condensed Matter

Rossen Dandoloff

2.1 Topology

2.1.1 Introduction

There is an old joke among mathematicians. It goes that way [1]: A mathematician was asked: What is a topologist? Someone for whom there is no difference between a doughnut and a coffee cup with a handle.

In general, topology studies continuum properties of spaces that are not affected by continuous deformations. Such deformations may be e.g. stretching and bending. Obviously e.g. cutting and gluing do not belong to the allowed deformations. Usually these properties are studied on what is called topological spaces i.e. a collection of subspaces that are open sets. These open sets satisfying certain conditions represent a topological space. Some of the most important topological properties are (a) connectedness, which simply counts the number of holes in the space and (b) compactness which means a subset of the Euclidean space that is closed and bounded; closed means that it contains all its boundary points and bounded means that all its points are at some distance to a given point that is less than some fixed maximal distance. Some examples a given by a closed interval, a rectangle, an ellipse circle, a sphere or a finite set of points. An ellipse e.g. is topologically equivalent to a circle (into which it can be deformed by continuous deformation e.g. stretching) and a sphere is equivalent to an ellipsoid. Similarly, the set of the numbers 0, 4, 6 and 9 are topologically equivalent - they have one hole each. The numbers 1, 2, 3, 5 and 7 are also topologically equivalent - they have 0 holes each and the number 8 (has two holes) is not topologically equivalent to either set of numbers.

R. Dandoloff (✉)
Laboratoire de Physique Théorique et Modélisation, Université de Cergy-Pontoise, 95302 Cergy-Pontoise, France
e-mail: rdandoloff@yahoo.com

S. Gupta and A. Saxena (eds.), *The Role of Topology in Materials*,
Springer Series in Solid-State Sciences 189,
https://doi.org/10.1007/978-3-319-76596-9_2

In fact topology is the newest branch of geometry. It studies different sorts of spaces and especially the question what distinguishes different geometries. Felix Klein has suggested that the allowed transformations that keep certain kind of geometry unchanged is in fact its main mark. For example in the ordinary Euclidean geometry one is allowed to translate and rotate different objects, but bending and stretching are not allowed. Projective geometry on the other hand recognises different views of the same object as an allowed "transformation" within the projective geometry. The circle and the ellipse are projectively equivalent: all depends on the point of observation of a circle that may look like a circle or as an ellipse. Topology allows any continuous transformation that is reversible in a continuous way. Let us take the ellipse - it is equivalent to a circle or a square because one can continuously transform it into a circle or a square in a reversible way. If during the transformation one needs to cross two lines this is not any more a reversible transformation: an example is the Fig. 2.8. Topology as the almost most fundamental form of geometry is used in almost all branches of mathematics. It turns out that there is an even more fundamental form of geometry - the homotopy theory. It was formulated around 1900 by Poincare. Two geometric objects are called homotopic if they can continuously be transformed from one into the other without cutting and gluing. The number of allowed transformations is very big and one can deal with them as it is done in algebra. One can use homotopy to classify different geometrical objects and there are many applications to physics too: spin systems, liquid crystals etc.

Here we will start with the application of homotopy to physics. In order to do this we will use the notion of *order parameter* which is widely used in physics. The order parameter is usually a geometric object (unit vector, tensor etc.) which best characterizes the state of the physical material that we are studying. For example if we are studying a three dimensional ferromagnet, the most important property is its magnetization, which is represented by an unit vector field. The unit vectors of this vector field may point in any direction (at sufficiently high temperature where the magnets are not oriented in any particular direction). These vectors may be mapped to a unit sphere as shown on the Fig. 2.1. The unit sphere is called a *target space*. If the ferromagnet is two dimensional, and the magnetization vectors lye in the plane, then the target space is a circle with unit radius.

In order to fully take advantage of the topology and the mapping from the physical to the order parameter space, we will introduce the so called *compactification* of the physical space. Let us explain this on a simple example. Consider a two dimensional plane with a ferromagnet field on it which at the infinity points to the same direction, say perpendicular to the plane and upward. From the point of view of the ferromagnetic field the infinity of the physical plane is characterized by only one single vector that points up. So, we may bring al the infinity in one point, but then our physical plane will look like a sphere where the north pole of the sphere is the point which represents the infinity of the plane.

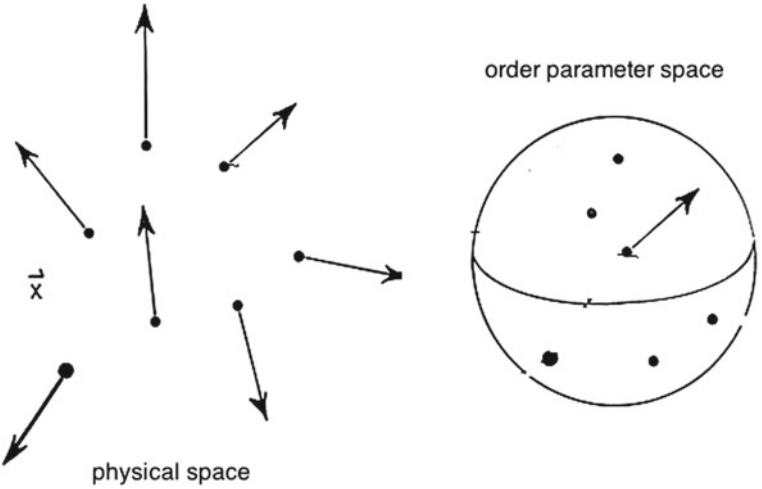

Fig. 2.1 Mapping from physical space to order parameter space

2.1.2 *Classification of Vector Fields with Homogeneous Boundary Conditions*

The mapping from the compactified physical space (e.g. the sphere S^2) onto the target space (S^2 in the case of the ferromagnetic field), allows to classify the different vector field configurations into separate *homotopy* classes. The notation is the following:

$$\pi_2(S^2) = \pi_2(S^2) = \mathbf{Z}(the\ group\ of\ the\ relative\ integers) \tag{2.1}$$

where $n = 0, 1, 2, \ldots$ is an integer which labels the corresponding vector field configuration. Equation (2.1) means how many times the sphere may wrap another sphere. As an example let us consider $n = 1$ - this configuration is such that the mapping of the vector field on the target space covers the sphere S^2 just once, for $n = 2$ the target space S^2 has been covered twice. It is clear now that it is not possible by continuous transformation to deform the configuration with $n = 1$ (here the tips of the vectors mapped onto the target space cover the sphere once) into configuration with $n = 2$ (here the tips of the vectors mapped onto the sphere cover S^2 twice).

Let us consider now an one dimensional physical space (an infinite line) with a ferromagnetic field (a unit vector field) on it. We will consider first a magnetization which lies in the plane perpendicular to the line, i.e. the magnetisation vector may point in any direction perpendicular to the physical line. It is obvious now that the target space is an unit circle S^1. If the boundary conditions are homogeneous i.e. the magnetisation vectors at + infinity and at − infinity of the physical line, are parallel, then we may compactify the line into a circle. Now the different homotopy classes of configurations are given by the following equation:

$$\pi_1(S^1) = \pi_2(S^2) = \mathbf{Z} \tag{2.2}$$

This equation tells us how many times the circle may wrap around another circle. The class $n \in \mathbf{Z}$ means that the magnetization vector points at the same direction at $\pm\infty$ and turns once around the line going from $-\infty$ to $+\infty$. Let us note however that not all spin configurations with homogeneous boundary conditions lead to different homotopy classes. As an example let us take the line with spins that may point in any direction i.e. the target space now is s^2. Now the topological classification is given by the following homotopy:

$$\pi_1(S^2) = 0 \tag{2.3}$$

Here any closed curve (the mapping from the circle to the surface of the sphere) on S^2 may be shrunk to a point.

2.1.3 *Classification of Defects in Vector Fields (Mainly Spin Fields)*

In order to better illustrate the role of topology in the classification of defects [2] we will concentrate only on two dimensional spin fields where spins lye in the plane i.e. the target space is the circle S^1. The case of spin fields (vector fields) may be generalised to describe liquid crystals as well as there the order parameter is a headless vector. Now, here the idea is to surround the defect by a closed contour and to map the vectors on that contour onto the target space, see Fig. 2.2. On Fig. 2.2 we see that the closed curve on target space may be shrunk to a point. This means that there is no defect inside the loop. The situation would have been different if the vector field on the circle would have been radial in any point - then the closed curve on the target space would have wrapped once the circle and the result would have been the following homotopy equation:

$$\pi_1(S^1) = \pi_2(S^2) = \mathbf{Z} \tag{2.4}$$

The defect here represents a source of the vector field. On the other hand if the vector field is allowed to come out of the plane, the target space becomes S^2 and as we have seen, any closed curve on the sphere can continuously be shrunk to a point, meaning that there is no defect enclosed by the loop on the plane.

2.1.4 *Defects and Homogeneous Boundary Conditions*

Let us for a moment come back to our discussion of homogeneous boundary conditions and see what does it mean in view of the preceding discussion of topological

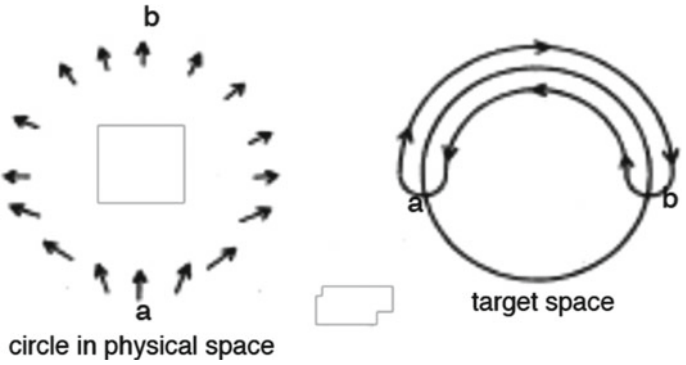

Fig. 2.2 Mapping from a closed contour around the defect to the order parameter space

classification of defects. If we consider the plane as our physical space, the homogeneous boundary condition for a vector field on it means that a loop at infinity (where the vectors point all in the same direction) will map to a single point on the target space. Now, let us suppose that there is a point defect somewhere on the plane. If we draw a closed loop around this defect and map the vectors on the target space we will get a closed line which we will not be able to shrink to a point. We may deform our loop on the physical plane to a loop at infinity and the map on the target space would not be shrinkable to a point. This contradiction tells us that imposing homogeneous boundary conditions also means that we exclude all point defects from the vector field.

2.2 Geometry

2.2.1 Energy

So far we have seen that very often spin fields with homogeneous boundary conditions fall into different homotopy classes. Now we will see what is the consequence for the energy of these different classes. For simplicity let us consider a ferromagnetic field – the energy is lowest when all vectors are parallel.

We will consider first the plane R^2 which represents the simplest 2D manifold. We will impose on the vector field on R^2 homogeneous boundary conditions: $lim_{r\to\infty}\vec{n} \to \vec{n}_0$. With these boundary conditions we may compactify the plane into the sphere S^2. Now the vector field configurations that may appear on the plane may be classified in homotopy classes $\pi_2(S^2) = \mathbf{Z}$ [3]. This topological classification in general is not related to the energy of the system. We may write the Hamiltonian for the vector field on R^2 as follows:

$$H = \int (\nabla \vec{n})^2 d^2x, \quad \vec{n}^2 = 1. \tag{2.5}$$

Nevertheless topology does give some indications about the energy of a field configuration in each homotopy class of equivalence using the Bogomolny inequalities [4]:

$$(\partial_i \vec{n} - \epsilon_{ij} \partial_j \vec{n})^2 \geq 0, \tag{2.6}$$

and therefore

$$H \geq \int \vec{n} \cdot (\partial_x \vec{n} \wedge \partial_y \vec{n}) dx dy. \tag{2.7}$$

It is obvious from (2.6) that when

$$\partial_i \vec{n} = \pm \epsilon_{ij} \partial_j \vec{n}. \tag{2.8}$$

minimum energy is reached in each class. Equation (2.8) are called "self-dual equations". Homotopy is useful for establishing different classes of vector field configurations and may help establish some inequalities regarding the energy in each configuration but geometry in general is not much more helpful in establishing the energy of a field configuration. Especially a geometry without an internal length (this is the case e.g. for the plane R^2). Nontrivial filed configurations on the plane R^2 may be scaled (shrunk) to a point without affecting the energy of the configuration. This happens because the Hamiltonian is symmetric under homothety (stretching of the space). Let us consider what happens with the Hamiltonian under stretching of the space by a factor λ: $x \to \lambda x$ and $y \to \lambda y$

$$E_\lambda = \int \int \left(\left(\frac{\partial n}{\partial \lambda x} \right)^2 + \left(\frac{\partial n}{\partial \lambda y} \right)^2 \right) d\lambda x d\lambda y = \int \int \left(\left(\frac{\partial n}{\partial x} \right)^2 + \left(\frac{\partial n}{\partial y} \right)^2 \right) dx dy = E. \tag{2.9}$$

The energy of the field configuration is invariant under stretching. As we mentioned above this means that the whole configuration may be shrunk into a point. These topological configurations are energetically metastable. The deeper reason for this to happen is that there is no internal length (or characteristic length) in the problem. Naturally there is no length in topology.

2.2.2 *Geometry with Intrinsic Length: The Cylinder*

As a geometry with intrinsic length we will consider the cylinder. The intrinsic length of the cylinder is its radius ρ_0. We will consider a cylindrically symmetric vector field (spin field) on the cylinder with radius ρ_0. As an immediate consequence of the presence of the intrinsic length ρ_0 we note that the homothety does not apply here and the

energy does depend on ρ_0. The order parameter for the classical Heisenberg model is the unit vector which covers the sphere S^2. It is easier to work with the Euler angles θ and ϕ on the unit sphere because they incorporate the constraint ($\mathbf{n}^2 = 1$). Our independent vector fields will be (θ, Φ) where $\vec{n} = (\cos\theta,\ \sin\theta\ \cos\Phi,\ \sin\theta\ \sin\Phi)$. Here θ is the co-latitude and Φ is the azimuthal angle. In cylindrical coordinates (ρ, x, φ) we can write the Hamiltonian in the following way [5]

$$H_{isotropic} = J \iint_{cylinder} \left[(\partial_x \theta)^2 + \sin^2\theta\ (\partial_x \Phi)^2 + \frac{(\partial_\varphi \theta)^2}{\rho_0^2} + \frac{\sin^2\theta}{\rho_0^2} (\partial_\varphi \Phi)^2 \right] \rho\, dx d\varphi, \tag{2.10}$$

where J is the spin-spin coupling constant.

We will consider our vector field with homogeneous boundary conditions at both ends of the cylinder, because then we can compactify the cylinder using topological considerations. Homogeneous boundary conditions in this case mean $\lim_{x\to\infty} \theta \equiv 0[\pi]$. We ask also that $\lim_{x\to\infty} \frac{d\theta}{dx} = 0$. This second condition is required in order to have finite energy on the infinite cylinder. The fact that $\frac{d\theta}{dx}$ goes to zero should insure the convergence of the integral in (2.10). With the homogeneous boundary conditions at both ends of the cylinder we can make coinside all points at infinity and compactify the infinite cylinder into a sphere (the ends of the cylinder become the two poles of the sphere). Then we can map the sphere (the compactified cylinder) onto S^2 (the order parameter manifold) and so we get $\pi_2(S^2) = \mathbf{Z}$. The result is that the spin configurations on the infinite cylinder can be classified in different classes of topologically non-trivial spin distributions [3, 5]. Inside each class, the spin configurations are topologically equivalent because they belong to the same homotopy class.

In this example we will consider only solutions with cylindrical symmetry. They will be sufficient for our purposes. For the angles θ and Φ the following conditions must apply:

$$\Phi = \varphi \quad , \qquad \frac{\partial\theta}{\partial\varphi} = 0. \tag{2.11}$$

The Hamiltonian (2.10) then becomes

$$H_{isotropic} = 2\pi\rho_0 J \int_{-\infty}^{+\infty} \left[\left(\frac{d\theta}{dx} \right)^2 + \frac{\sin^2\theta}{\rho_0^2} \right] dx. \tag{2.12}$$

After variation of the Hamiltonian $\delta H = 0$, the Euler–Lagrange equation leads to

$$\frac{d^2\theta(x)}{dx^2} = \frac{1}{2\rho_0^2} \sin 2\theta. \tag{2.13}$$

This equation represents the sine-Gordon equation whose solutions are solitons. This second order differential equation appears in a big variety of physical prob-

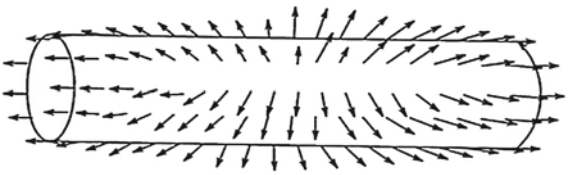

Fig. 2.3 Cylindrically symmetric $0 \to \pi$ twist soliton on an infinite cylinder

lems e.g. charge-density-wave in different materials, splay waves on membranes, Bloch wall motion in magnetic crystals, magnetic flux in Josephson lines, propagation of dislocations in crystals, torsion coupled pendula, two-dimensional models of elementary particles, etc.

One solution for a configuration which belongs to the first homotopy class and representing a single spin twist, is given by:

$$\theta = 2 \arctan \exp \frac{x}{\rho_0}. \tag{2.14}$$

A schematic representation is given in Fig. 2.3 The characteristic length ρ of the cylinder appears explicitly in the solution. In this solution ρ_0 represents the width of the twist soliton.

2.2.3 Geometry with Intrinsic Length: Plane with a Disc Missing

Now we will consider yet another example of a geometry with intrinsic length namely a non simply connected plane R^2. Here the intrinsic length will be the radius ρ_0 of the disk $D^2_{\rho_0}$ cut off from the plane. First we will consider spins on $R^2 \backslash D^2_{\rho_0}$ and then the same classical spin field but in a perpendicular to the plane magnetic field **B**. In a cylindrical coordinate system (ρ, ϕ) he Hamiltonian (the nonlinear sigma model) reads:

$$H = 2\pi \int_{\rho_0}^{\infty} d\rho \left[\rho \theta_\rho^2 + \frac{\sin^2 \theta}{\rho} \right]. \tag{2.15}$$

Here we are using the Euler angles representation for the unit vector $\mathbf{n} = (\sin\theta \cos\Phi, \sin\theta \sin\Phi, \cos\theta)$, (the spins lie on a unit sphere S^2). Without loss of generality we will assume cylindrical symmetry for the spin configurations: $\theta = \theta(\rho)$ and $\Phi = \phi$. The solutions of the Euler–Lagrange (EL) equation will give the configurations with lowest energy:

$$\theta_\rho + \rho \theta_{\rho\rho} = \frac{\sin\theta \cos\theta}{\rho}. \tag{2.16}$$

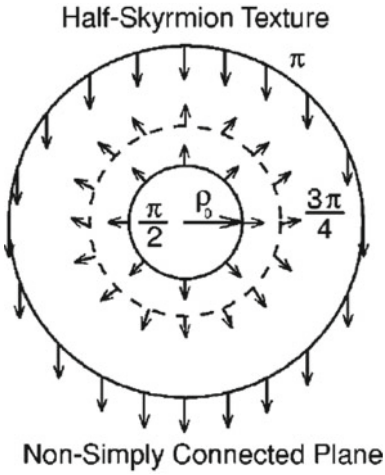

Fig. 2.4 Field on a plane with a disc missing

Here we take $\theta(\rho_0) =$ constant. and define a new radius coordinate $\overline{\rho} = \ln(\rho/\rho_0)$ which will allow us to reduce the EL equation to a simple sine-Gordon equation:

$$\theta_{\overline{\rho}\overline{\rho}} = \frac{\sin 2\theta}{2}. \tag{2.17}$$

A novel exact half-skyrmion appears to be the solution of this sine-Gordon equation on the non-simply connected plane shown on Fig. 2.4.

$$\theta(\rho, \rho_0) = 2\tan^{-1}\frac{\rho}{\rho_0}. \tag{2.18}$$

This solution depends on ρ_0, the intrinsic length in the problem and can not be shrunk to a point like the usual Belavin-Polyakov skyrmion [3]. It is located at $\rho_c = \rho_0 \cot(\pi/8) = \rho_0(1+\sqrt{2})$ with energy 4π (instead of 8π) and topological charge density

$$q(\rho) = \frac{\theta_\rho \sin\theta}{4\pi\rho} = \frac{1}{\pi}\frac{\rho_0^2}{(\rho^2+\rho_0^2)^2}. \tag{2.19}$$

Equivalently, the components of the unit vector field are:

$$n^x = \frac{2x\rho_0}{\rho^2+\rho_0^2}, \quad n^y = \frac{2y\rho_0}{\rho^2+\rho_0^2}, \quad n^z = \frac{\rho^2-\rho_0^2}{\rho^2+\rho_0^2}. \tag{2.20}$$

2.2.4 Interaction Between Geometry and Physical Field

We have seen so far that the intrinsic length of the underlying manifold appears in the solutions for the vector field distributions i.e. the underlying manifold influences the vector field. The opposite is true too. In order to illustrate this we will turn our attention to yet another exact solution of the sine-Gordon equation. We will consider now a periodic solution of this equation which represents a the soliton lattice [6]. We note here that the Bogomol'nyi argument can be applied for any period (for which the unit vector covers S^2) of this periodic solution. We note here that for one period on the rigid cylinder the self-dual equations (2.6) are still valid and therefore any function that satisfies (2.6) will satisfy the sine-Gordon equation as well (2.13). The periodic solution of the sine-Gordon equation is given by:

$$\theta = \arccos\left[\mathrm{sn}\left(\frac{x}{k\rho_0}, k\right)\right]. \tag{2.21}$$

Let us discuss this periodic solution. The constant k is the modulus of the Jacobi elliptic function sn (sine-amplitude); the period of the solution is given by $4d = 4\rho_0 k K(k)$ where here $K(k)$ is the complete elliptic integral of the first kind. The periodic solution transforms into the single twist soliton (2.14) solution of the sine-Gordon equation In the limit $k \to 1$, as $\lim_{k\to 1} K(k) \to \infty$, the half period $2d$ tends to infinity and at the the boundaries, we get the homogeneous conditions we have discussed in Sect. 2.2. We can now calculate the energy per soliton (over half period $2d$, as $\theta(\pm d) \equiv 0[\pi]$):

$$H_{isotropic} = \frac{8\pi J}{k}\left[E(k) - \frac{k'^2 K(k)}{2}\right], \tag{2.22}$$

In this equation k' is the complementary modulus ($k'^2 = 1 - k^2$) and $E(k)$ is the complete elliptic integral of the second kind. In the low soliton density limit, i.e. $k \to 1$ [then $E(k) \to 1$], we can expand the exact solution (2.22) and obtain the energy per soliton which reads:

$$H_{isotropic} = 8\pi J + 32\pi J exp\left(-\frac{2d}{\rho_0}\right) + \ldots = 8\pi J + 2\pi J k'^2 + \ldots . \tag{2.23}$$

The first term in this expansion represents the self energy of a soliton over one period (which corresponds to a soliton that stretches from $-\infty$ to $+\infty$. The second term represents an additional energy that corresponds to the repulsive interaction between solitons. The periodic solution (2.21) is an exact solution of the sine-Gordon equation but nevertheless does not satisfy the self duality equations and that is the reason why the energy per soliton in the periodic solution does not reach the minimum energy per soliton $H^1_{isotropic} = 8\pi J$. For a single soliton on a cylinder we have some sort of "equipartition" relation ${\rho_0}^2\ (\partial_x\theta)^2 = \sin^2\theta$ between "kinetic" energy on the

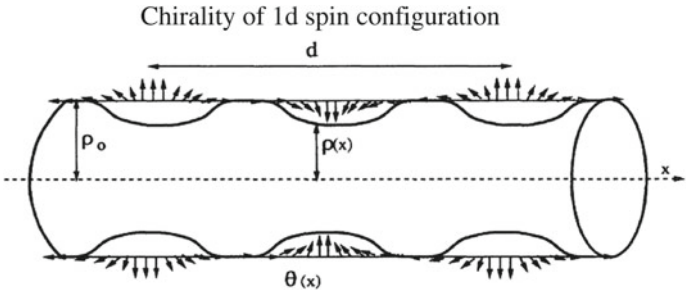

Fig. 2.5 Periodic spin soliton and periodic deformation of the cylinder

left and "potential" energy on the right. For the periodic solution the corresponding relation is:

$$\rho_0{}^2\ (\partial_x\theta)^2 = \sin^2\theta + \frac{k'^2}{k^2}. \tag{2.24}$$

Now we see that on the right hand side of this equation there is an additional "potential" energy $(\frac{k'}{k})^2$ that corresponds to an exponential repulsive interaction between the solitons. The soliton likes to stretch from $-\infty$ to $+\infty$ but the presence of additional soliton does not allow this to happen - this is the geometric frustration that appears in this case. In the limit of a single twist soliton ($d \to \infty$ and $k' = 0$) $(\frac{k'}{k})^2 = 0$ and we get the energy $H^1_{isotropic}$ of the single twist soliton: the interaction term vanishes. There is another possibility that may allow us to diminish the magnetic energy per soliton on the cylinder. If we allow the cylinder to deform as shown on Fig. 2.5 this will diminish the magnetic energy per soliton but will require some elastic energy for the deformation of the cylinder. Allowing for elastic deformations of the cylinder means that ρ will become x-dependent which will modify the Hamiltonian and the associated equations as discussed in [6].

2.2.5 Chirality of 1d Spin Configurations

We have seen that the usual homotopy classification of Heisenberg spins (target space is S^2) in one dimension is trivial: $\pi_1(S^2) = 0$. However, there is another non-trivial topological classification of Heisenberg spins based on chirality [7]. In order to find out if there are other topological structures in the one dimensional case one has to better analyse the Heisenberg hamiltonian. As the vector field is normalised to unity we once again will use the Euler angles representation for $\mathbf{n} = (\sin\theta\cos\phi, \sin\theta\sin\phi, \cos\theta)$. Using θ and ϕ variables the hamiltonian can be written in the following form:

$$H = J \int_{-L}^{+L} (\theta_s^2 + \sin\theta^2 \phi_s^2) ds \tag{2.25}$$

here s stands for $\frac{d}{ds}$ and s represents the coordinate along R^1. This hamiltonian is not invariant under homothety transformation $s \to \lambda s$ and that's why the spin configurations are not metastable like in the $2D$ case. The equations of motion for this spin hamiltonian have been established by Tjon and Wright [8] where ϕ and $\cos\theta$ represent the conjugated generalised coordinate and momentum. The Poisson bracket gives $[\phi(x), \cos\theta(y)] = \delta(x - y)$. Here the generator of translations (momentum) is given by the following expression:

$$P = \int_{-L}^{+L} (1 - \cos\theta)\phi_s ds \tag{2.26}$$

The momentum operator verifies the Poisson brackets: $[\phi(s), P] = -\phi_s$ and $[\cos\theta(s), P] = -\frac{d}{ds}\cos\theta(s)$ [8]. It turns out that P is a constant of the motion for this Hamiltonian [8].

Now, for our analysis of the possible spin configurations we will map the unit vector $\mathbf{n}$ to the unit tangent of a space. Now, it turns out that different space curves represent different spin configurations. Here the boundary conditions we will use are that at $\pm L$ the spins will be parallel. In this case different curves representing different spin configurations will tend to a straight line as $s \to \pm L$. Of special interest for us is the writhe of a curve (which characterises its chirality of the). For a closed curve it is defined as follows [9]:

$$Wr = \frac{1}{4\pi} \oint ds \oint ds' \frac{(\mathbf{r}(s) - \mathbf{r}(s').(\mathbf{n}(s) - \mathbf{n}(s'))}{|\mathbf{r}(s) - \mathbf{r}(s')|^3} \tag{2.27}$$

In this case we distinguish two classes of homotopy equivalent curves: one where two ends of the curve are rotated to each other by 2π and the other where the two ends are rotated by 4π. The reason for the appearance of these two classes is the fact that the group $SO(3)$ is non simply connected manifold and closed loops in $SO(3)$ fall into two classes: those who can be contracted to a point and those for which this is impossible. For example a triad evolving on such a space curve from $s = -L$ to $s = L$ traces out a closed curve on $SO(3)$ [10]

We will apply a theorem by Fuller which allows to express Wr as an integral of a local quantity. We will express Wr with respect to a reference curve C_0 (which for simplicity is taken to be a straight line):

$$Wr = Wr_0 + \frac{1}{2\pi} \int_{-L}^{+L} \frac{\mathbf{n}_0 \times \mathbf{n}.\frac{d}{ds}(\mathbf{n}_0 + \mathbf{n})}{(1 + \mathbf{n}_0.\mathbf{n})} ds \tag{2.28}$$

here Wr_0 is the writhe of the reference curve. A simple calculation gives the following expression for the writhe:

$$Wr = \frac{1}{2\pi}\int_{-L}^{+L}(1-\cos\theta)\phi_s ds \tag{2.29}$$

Let us note here that the writhe Wr for the spin configurations (quantity that characterises the chirality of the spin configuration) coincides with the total momentum P. We have seen that the total momentum P is a conserved quantity - it follows that Wr is a conserved quantity too. This will lead us to a new class of possible excitations for the continuous classical spin Heisenberg model. The ground state configuration is represented by $\theta = 0$ and let us note that the curves whose ends are rotated by 4π also belong to the same class of configurations [10]. In order to calculate the lower bound for the energy of a configuration that doesn't belong to the ground state configuration (curves whose ends are rotated by 2π) we need closed curves. Let us take first a space curve representing a spin configuration that goes from $-L$ to $+L$. This curve is completed by a straight line between $-L$ and $-\infty$ and between $+L$ and $+\infty$ and is closed by a semi-circle at infinity in order to form a closed curve. Note that on the straight segments and on the semi-circle at infinity the curvature k is zero. The writhe is zero for the straight segments when $s \in \pm(L,\infty)$ as well as for the infinite semi-circle. This geometrical construction does not change the writhe of the actual curve. Such a curve belongs to a whole class of configurations which deform smoothly from one to another and who are separated from the ground state class by a jump in the writhe Wr. Let us first note that for closed curves [11]:

$$\oint k ds \geq 2\pi \tag{2.30}$$

We note that the curvature $k \neq 0$ only for $s \in (-L,+L)$, and then the above inequality is equivalent to:

$$\int_{-L}^{+L} k ds \geq 2\pi \tag{2.31}$$

We will use the following Cauchy–Schwarz inequality:

$$\left(\int_{-L}^{+L} k ds\right)^2 \leq 2L\int_{-L}^{+L} k^2 ds \tag{2.32}$$

and the following expression for the curvature in Euler angles: $k^2 = \theta_s^2 + \sin^2\theta\phi_s^2$. Then we can present the following obvious inequality for the energy of the spin chain:

$$H = J\int_{-L}^{+L}(\theta_s^2+\sin^2\theta\phi_s^2)ds = J\int_{-L}^{+L}k^2 ds \geq \frac{J\left(\int_{-L}^{+L}k ds\right)^2}{2L} \geq J\frac{4\pi^2}{2L} = J\frac{2\pi^2}{L} \tag{2.33}$$

The energy is limited from below for this class of configurations for which both ends of the representing space curve are rotated at 2π. It is clear that for an infinite chain

$L \to \infty$ the lower bound goes to 0. On the other hand the barrier which separates P from the zeroth class remains. The above result is consistent with the inequality for the elastic energy of thin rod whose ends are rotated by 2π relative to each other [10] where the result is based on the same property of the rotation group $SO(3)$. In this case the thin rod has only bending rigidity J and no torsional rigidity.

2.3 Quantum Potential, Thin Tubes, Knots

Yet another interesting application of geometry concerns quantum theory. Especially the appearance of induced quantum potential on curved surfaces and on curves (thin tubes) (the effective potential that appears on curved surfaces or membranes is $V_{eff} = -\frac{\hbar^2}{2m}(M^2 - K)$ where $K = k_1 k_2$ is the Gaussian curvature and k_1 and k_2 are the sectional curvatures and $M = 1/2(k_1 + k_2)$ is the mean curvature and the effective potential on curves or in thin tubes is $V_{eff} = -\frac{\hbar^2}{2m}\frac{k^2}{4}$, where k is the curvature of the axis of the tube [12]. We will briefly discuss the appearance of quantum potential in a thin tube and give a "hand-waving" argument in favour of it. The argument is based on Heisenberg's uncertainty principle, see Fig. 2.6.

It is the obvious that as $\Delta p_s \leq \Delta p_x$, the corresponding energies are related as follows: $E_s = \frac{\Delta p_s^2}{2m} \leq E_x = \frac{\Delta p_x^2}{2m}$.This shows that the free particles prefer to be localised in the bent region of the thin tube.

Let us now, as an example, consider a trefoil knot (knots appear often in polymers). It has turned out that one may create a qubit using the geometry of a tight trefoil knot [13].

In mathematics knots are represented as closed, self-avoiding *curves* embedded in a three-dimensional space. Any knot can be tied on a thread (or a curve) of any length and when we pull on both ends of the thread the knot transforms into a point which means that all conformations are essentially equivalent. Yet another problem is the lack of characteristic length with does not allow for the introduction of energy scale. Physics deals with real material knots. The thread has a finite diameter and pulling the thread on both ends does not transform the knot into a point. The diameter of the physical thread plays the role of a characteristic length.

In our example we will use a trefoil knot where the thread will have a circular cross-section with a finite radius. Then we will pull the knot tight. At some point we

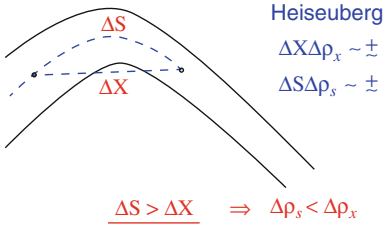

Fig. 2.6 Bent thin tube

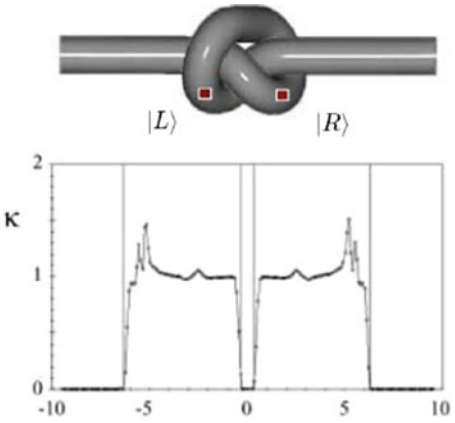

Fig. 2.7 Tight open knot and the curvature of its center ligne

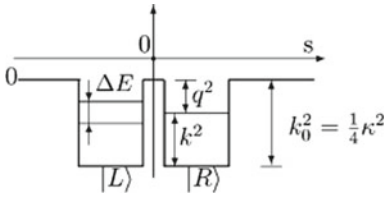

Fig. 2.8 A double well potential for the tight trefoil knot

will note that we can not pull any further without changing the cross-section of the knot. The final confirmation we have reached is called *tight open knot*. We may get a *tight closed knot* simply by "gluing" together the loose ends of the *tight open knot*. As seen on Fig. 2.7 there is a plane of symmetry which separates the left from the right part of the trefoil knot. This most symmetrical conformation of the trefoil knot appears to be also the most energetically (elastic energy) favourable.

There is no analytical expression for the curvature of the center line of a tight knot, but there are experimental measurement, which are presented on Fig. 2.7 [14]. There is compete left-right symmetry of the curvature and there is a flat region ($k = 0$) in the middle.

As we have seen, the curvature of a space curve or the centerline of a thin tube is related to the induced quantum potential. The curvature presented in Fig. 2.8 can be modelled to represent the following double well potential for the tight knot. See Fig. 2.8. Finally the tuneling possibility between the two wells splits the localised level into two and so the tight trefoil knot represents quantum mechanically a two level system which may be used as a microscopic qubit.

The combination of curved and straight nanobars may produce the same double well potential as shown in Fig. 2.8. One such combination is shown in Fig. 2.9. The possibility to create almost any given quantum potential using a combination of suitable curved nanobars is very big.

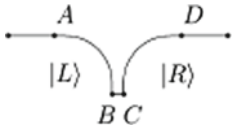

Fig. 2.9 Circular and straight nanobars create a double-well potential

The sectors $A-B$ and $C-D$ represent a quarter of a circle ($V_{eff.} = -\frac{\hbar^2}{2m}\frac{k_0^2}{4}$, with $k_0 = \frac{1}{r_0}$, where r_0 is the radius of the circle) and the sector $B-C$ is a straight line ($V_{eff.} = 0$).

2.4 Conclusions

By using topology and geometry we established a link between the order parameter of the concrete material and the underlying geometry and make predictions regarding the bounds of energy imposed by topological and geometrical constraints without solving the very complicated equations of motion. Classification of defects in different materials is also possible. This is true for the classical as well as for the quantum level of consideration. Further investigations on the quantum level, using topology, may include the quantum effective potential which is geometric in its nature and may play an important role in understanding of some properties of nanostructures. Finally we mention that topology and geometry can not replace solving of the microscopic equations of motion but may bring additional insights for the understanding of the fundamental properties of matter.

References

1. P. Renteln, A. Dundes, Foolproof: a sampling of mathematical folk humor. Not. Am. Math. Soc. **52**, 24–34 (2005)
2. G. Toulouse, M. Kleman, J. Phys. Lett. (Paris) **37**, L-149 (1976); M. Kleman, L. Michel, G. Toulouse, J. Phys. Lett. (Paris) **38**, L-195 (1977)
3. A.A. Belavin, A.M. Polyakov, JETP Lett. **22**, 245 (1975)
4. E.B. Bogomol'nyi, Sov. J. Nucl. Phys. **24**, 449 (1976)
5. S. Villain-Guillot, R. Dandoloff, A. Saxena, Phys. Lett. A **188**, 343 (1994)
6. R. Dandoloff, S. Villain-Guillot, A. Saxena, A. Bishop, Phys. Rev. Lett. **74**, 813 (1995)
7. R. Dandoloff, Adv. Condens. Matter Phys. **2015** (2015). (Article ID 954524)
8. J. Tjon, J. Wright, Phys. Rev. B **15**, 3470 (1977)
9. M.D. Frank-Kamenetskii, A.V. Vologodskii, Sov. Phys. Usp. **24**(8), 679 (1981)
10. J. Baez, R. Dandoloff, Phys. Lett. A **155**, 145 (1991)
11. W. Fenchel, Math. Ann. **10**, 238 (1929)
12. R.C.T. da Costa, Phys. Rev. A **23**, 1982 (1981)
13. V. Atanasov, R. Dandoloff, Phys. Lett. A **373**, 716 (2009)
14. P. Pieranski, S. Przybyl, A. Stasiak, Eur. J. Phys. E **6**, 123 (2001)